

Matching IR-MALDI-o-TOF Mass Spectrometry with the TLC Overlay Binding Assay and Its Clinical Application for Tracing Tumor-Associated Glycosphingolipids in Hepatocellular and Pancreatic Cancer

Ute Distler,[†] Marcel Hülsewig,[†] Jamal Souady,[†] Klaus Dreisewerd,[†] Jörg Haier,[‡] Norbert Senninger,[‡] Alexander W. Friedrich,[§] Helge Karch,[§] Franz Hillenkamp,[†] Stefan Berkenkamp,^{||} Jasna Peter-Katalinić,[†] and Johannes Müthing^{*†}

Institute of Medical Physics and Biophysics and Institute for Hygiene, University of Münster, D-48149 Münster, Germany, Department of General Surgery, Münster University Hospital, D-48149 Münster, Germany, and Sequenom GmbH, D-22761 Hamburg, Germany

Glycosphingolipids (GSLs), composed of a hydrophilic carbohydrate chain and a lipophilic ceramide anchor, play pivotal roles in countless biological processes, including the development of cancer. As part of the investigation of the vertebrate glycome, GSL analysis is undergoing rapid expansion owing to the application of modern mass spectrometry. Here we introduce direct coupling of IR-MALDI-o-TOF mass spectrometry with the TLC overlay binding assay for the structural characterization of GSLs. We matched three complementary methods including (i) TLC separation of GSLs, (ii) their detection with oligosaccharide-specific proteins, and (iii) in situ MS analysis of protein-detected GSLs. The high specificity and sensitivity is demonstrated by use of antibodies, bacterial toxins, and a plant lectin. The procedure works on a nanogram scale, and detection limits of less than 1 ng at its best of immunostained GSLs were obtained. Furthermore, only crude lipid extracts of biological sources are required for TLC-IR-MALDI-MS, omitting any laborious GSL downstream purification procedures. This strategy was successfully applied to the identification of cancer-associated GSLs in human hepatocellular and pancreatic tumors. Thus, the in situ TLC-IR-MALDI-MS of immunolabeled GSLs opens new doors by delivering specific structural information of trace quantities of GSLs with only a limited investment in sample preparation.

Glycosphingolipids (GSLs) are amphipathic molecules, which are composed of a hydrophilic oligosaccharide chain and a hydrophobic ceramide moiety. In mammalian cells, the ceramide moiety is typically built up from the long-chain aminoalcohol

sphingosine (d18:1), which is linked with a fatty acid varying in chain length from C16 to C24. GSLs are located primarily in the outer leaflet of the plasma membrane of animal cells and are organized in microdomains^{1,2} or lipid rafts³ also referred to as glycosynapses.⁴ Their oligosaccharides protrude from the cell surface microdomains and function as recognition molecules,⁵ whereas the ceramide moiety operates as an intracellular regulator upon binding of extracellular ligands.⁶

GSLs are involved in countless biological events, including cell differentiation, cell adhesion, microbial pathogenesis, and immunological recognition.^{7–9} Clinically important, aberrant glycosylation occurs in essentially all types of human cancers.^{10,11} For example, neutral GSLs such as the Shiga toxin receptor globotriaosylceramide (CD77) or sialylated GSLs (=gangliosides) of the CD75s type constitute tumor-associated antigens, which are currently under clinical investigation as potential targets for anticancer therapies.^{12–15}

High-performance thin-layer chromatography (TLC) is widely used as an invaluable tool for the separation of GSLs in mixtures.^{16,17} In conjunction with carbohydrate-binding proteins such

* To whom correspondence should be addressed. Phone: +49-251-8355192. Fax: +49-251-8355140. E-mail: jm@uni-muenster.de.

[†] Institute of Medical Physics and Biophysics, University of Münster.

[‡] Münster University Hospital.

[§] Institute for Hygiene, University of Münster.

^{||} Sequenom GmbH.

- (1) Hakomori, S. *Glycoconjugate J.* **2000**, *17*, 143–151.
- (2) Sonnino, S.; Prinetti, A.; Mauri, L.; Chigorno, V.; Tettamanti, G. *Chem. Rev.* **2006**, *106*, 2111–2125.
- (3) Simons, T.; Toomre, D. *Nat. Rev. Mol. Cell. Biol.* **2000**, *1*, 31–41.
- (4) Hakomori, S. *Proc. Natl. Acad. Sci. U.S.A.* **2002**, *99*, 225–232.
- (5) Schnaar, R. L. *Glycobiology* **1991**, *1*, 477–485.
- (6) Hannun, Y. A.; Obeid, L. M. *Trends Biochem. Sci.* **1995**, *20*, 73–77.
- (7) Hakomori, S. *Glycoconjugate J.* **2000**, *17*, 627–647.
- (8) Karlsson, K. A. *Curr. Opin. Struct. Biol.* **1995**, *5*, 622–635.
- (9) Feizi, T. *Immunol. Rev.* **2000**, *173*, 79–88.
- (10) Feizi, T. *Nature* **1985**, *314*, 53–57.
- (11) Hakomori, S. *Proc. Natl. Acad. Sci. U.S.A.* **2002**, *99*, 10231–10233.
- (12) Gariepy, J. *Crit. Rev. Oncol. Hematol.* **2001**, *39*, 99–106.
- (13) Kovbasnjuk, O.; Mourtazina, R.; Baibakov, B.; Wang, T.; Elowsky, C.; Choti, M. A.; Kane, A.; Donowitz, M. *Proc. Natl. Acad. Sci. U.S.A.* **2005**, *102*, 19087–19092.
- (14) Habeck, M. *Drug Discovery Today* **2003**, *8*, 52–53.
- (15) Müthing, J.; Meisen, I.; Kniep, B.; Haier, J.; Senninger, N.; Neumann, U.; Langer, M.; Witthohn, K.; Milosević, J.; Peter-Katalinić, J. *FASEB J.* **2005**, *19*, 103–105.
- (16) Müthing, J. *J. Chromatogr., A* **1996**, *720*, 3–25.

as antibodies, lectins, or bacterial toxins, GSL species can be differentiated in overlay assays after separation by TLC. The TLC overlay assay introduced by Magnani et al.¹⁸ has been continuously optimized along with the fabrication of myriad monoclonal antibodies¹⁹ and the increasing availability of plant lectins and bacterial toxins directed to GSL determinants.^{20,21}

Mass spectrometry has become one of the most important technologies for the structural analysis of GSLs.^{22–24} In particular, electrospray ionization and matrix-assisted laser desorption/ionization mass spectrometry (MALDI-MS) allow highly sensitive characterization of GSL molecules by their molecular mass and sugar composition using fragmentation techniques and tandem MS/MS. Number and sequence of monosaccharides can be deduced for an unknown GSL by MS, but type of monosaccharides (e.g., galactose or glucose) and their anomeric configuration (α versus β) cannot be determined without auxiliary tools like glycosidases or carbohydrate-specific antibodies, lectins, and toxins or additional chemical investigations of purified GSLs by methylation analysis, gas chromatography, and others.²⁵

Direct coupling of MS with TLC, that is irradiation of TLC-separated analytes on the plate followed by MS analysis, has been reported in the past being especially attractive, because it provides chromatographic and at least partial structural information simultaneously.²⁶ Parallel TLC runs are required for conventional GSL staining or overlay binding assays using biological reagents, which allow direct comparison and thus a structural assignment of the GSL under MS investigation on the master TLC plate.^{27,28} TLC-MS, including MS analysis of GSLs transferred to synthetic membranes,^{29,30} has been consecutively improved,^{31–35} e.g., by decoupling of the desorption/ionization process in the ion source from the mass analysis as it is, for example, the case in orthogonal time-of-flight (o-TOF) MS.³⁶ We have employed this type of mass spectrometer with an infrared (IR) laser and applied it to the

compositional mapping of ganglioside, oligosaccharide, and phospholipid mixtures.^{37–39}

Here we describe the coupling of IR-MALDI-o-TOF-MS directly with the TLC overlay assay for the structural characterization of GSLs. We merged three complementary methods comprising (i) TLC separation of GSLs, (ii) their detection with oligosaccharide-specific proteins, and (iii) in situ analysis of overlay-detected GSLs by IR-MALDI-MS. The procedure works on a nanogram scale of GSLs with all carbohydrate-binding proteins so far investigated, and furthermore, it requires only crude lipid extracts from biological sources. We demonstrate as a medical important approach its application to the identification of cancer-associated GSLs in human tumors.

EXPERIMENTAL SECTION

Reference GSLs. A mixture of neutral GSLs, comprising lactosylceramide (Lc2Cer), globotriaosylceramide (Gb3Cer/CD77), and globotetraosylceramide (Gb4Cer), was prepared from human erythrocytes.⁴⁰ Neutral GSL references of neolacto and ganglio series were from human granulocytes and murine MDAY-D2 cell line, respectively.^{41,42} A ganglioside mixture containing as major compounds GM3(Neu5Ac), the CD75s-gangliosides IV⁶-Neu5Ac-nLc4Cer and VI⁶-Neu5Ac-nLc6Cer, and the isomeric iso-CD75s-gangliosides IV³-Neu5Ac-nLc4Cer and VI³-Neu5Ac-nLc6Cer, was isolated from human granulocytes as previously described.⁴³ A mixture of human brain gangliosides, composed of GM1, GD1a, GD1b, and GT1b, was purchased from Supelco Inc. (Bellefonte, PA). The neutral GSL and ganglioside core structures are listed in Table 1. The nomenclature of GSLs follows the IUPAC-IUBM recommendations 1997.⁴⁴ The symbolic representation system according to Varki⁴⁵ and the Consortium for Functional Glycomics⁴⁶ is used throughout this publication. All monosaccharides are in the D-configuration of the pyranose form and all glycosidic linkages originate from the C1 hydroxyl group except for sialic acids, which are linked from the C2 hydroxyl group.

Anti-GSL Antibodies. The specificity of the chicken polyclonal IgY antibody against neutral GSLs with Gal β 4GlcNAc residues (nLc4Cer, nLc6Cer, and nLc8Cer) has been previously reported.⁴⁷ The hybridoma cell line TIB 189 producing the monoclonal mouse IgM antibody 1B2-1B7 with Gal β 4GlcNAc-R specificity was obtained from the American Type Culture

- (17) Mùthing, J. In *Glycoanalysis Protocols*; Hounsell, E. F., Ed.; Methods in Molecular Biology 76: Humana Press Inc.: Totawa, NJ, 1998; pp 183–195.
- (18) Magnani, J. L.; Smith, D. F.; Ginsburg, V. *Anal. Biochem.* **1980**, *109*, 399–402.
- (19) Kannagi, R. *Methods Enzymol.* **2000**, *312*, 160–179.
- (20) Sharon, N.; Lis, H. *Glycobiology* **2004**, *14*, 53R–62R.
- (21) Sandvig, K.; van Deurs, B. *FEBS Lett.* **2002**, *529*, 49–53.
- (22) Peter-Katalinić, J. *Mass Spectrom. Rev.* **1994**, *13*, 77–98.
- (23) Costello, C. E. *Curr. Opin. Biotechnol.* **1999**, *10*, 22–28.
- (24) Levery, S. B. *Methods Enzymol.* **2005**, *405*, 300–369.
- (25) Hanisch, F.-G. *Biol. Mass Spectrom.* **1994**, *23*, 309–312.
- (26) Kushi, Y.; Handa, S. *J. Biochem.* **1985**, *98*, 265–268.
- (27) Kushi, Y.; Rokukawa, C.; Handa, S. *Anal. Biochem.* **1988**, *175*, 167–176.
- (28) Karlsson, K. A.; Lanne, B.; Pimlott, W.; Teneberg, S. *Carbohydr. Res.* **1991**, *221*, 49–61.
- (29) Taki, T.; Ishikawa, D.; Handa, S.; Kasama, T. *Anal. Biochem.* **1995**, *225*, 24–27.
- (30) Guittard, J.; Hronowski, X. L.; Costello, C. E. *Rapid Commun. Mass Spectrom.* **1999**, *13*, 1838–1849.
- (31) Chai, W.; Cashmore, G. C.; Carruthers, R. A.; Stoll, M. S.; Lawson, A. M. *Biol. Mass Spectrom.* **1991**, *20*, 169–178.
- (32) Chai, W.; Leteux, C.; Lawson, A. M.; Stoll, M. S. *Anal. Chem.* **2003**, *75*, 118–125.
- (33) O' Connor, P. B.; Budnik, B. A.; Ivleva, V. B.; Kaur, P.; Moyer, S. C.; Pittman, J. L.; Costello, C. E. *J. Am. Soc. Mass Spectrom.* **2004**, *15*, 128–132.
- (34) Ivleva, V. B.; Elkin, Y. N.; Budnik, B. A.; Moyer, S. C.; O' Connor, P. B.; Costello, C. E. *Anal. Chem.* **2004**, *76*, 6484–6491.
- (35) Nakamura, K.; Suzuki, Y.; Goto-Inoue, N.; Yoshida-Noro, C.; Suzuki, A. *Anal. Chem.* **2006**, *78*, 5736–5743.
- (36) Ivleva, V. B.; Sapp, L. M.; O' Connor, P. B.; Costello, C. E. *Am. Soc. Mass Spectrom.* **2005**, *16*, 1552–1560.

- (37) Dreisewerd, K.; Mùthing, J.; Rohlfing, A.; Meisen, I.; Vukelić, Ž.; Peter-Katalinić, J.; Hillenkamp, F.; Berkenkamp, S. *Anal. Chem.* **2005**, *77*, 4098–4107.
- (38) Dreisewerd, K.; Kölbl, S.; Peter-Katalinić, J.; Berkenkamp, S.; Pohlentz, G. *J. Am. Soc. Mass Spectrom.* **2006**, *17*, 139–150.
- (39) Rohlfing, A.; Mùthing, J.; Pohlentz, G.; Distler, U.; Peter-Katalinić, J.; Berkenkamp, S.; Dreisewerd, K. *Anal. Chem.* **2007**, *79*, 5793–5808.
- (40) Meisen, I.; Friedrich, A. W.; Karch, H.; Witting, U.; Peter-Katalinić, J.; Mùthing, J. *Rapid Commun. Mass Spectrom.* **2005**, *19*, 3659–3665.
- (41) Duvar, S.; Peter-Katalinić, J.; Hanisch, F.-G.; Mùthing, J. *Glycobiology* **1997**, *7*, 1099–1109.
- (42) Mùthing, J.; Burg, M.; Möckel, B.; Langer, M.; Metelmann-Strupat, W.; Werner, A.; Neumann, U.; Peter-Katalinić, J.; Eck, J. *Glycobiology* **2002**, *12*, 485–497.
- (43) Mùthing, J.; Unland, F.; Heitmann, D.; Orlich, M.; Hanisch, F.-G.; Peter-Katalinić, J.; Knäuper, V.; Tschesche, H.; Kelm, S.; Schauer, R.; Lehmann, J. *Glycoconjugate J.* **1993**, *10*, 120–126.
- (44) Chester, M. A. *Glycoconjugate J.* **1999**, *16*, 1–6.
- (45) Varki, A. *Nature* **2007**, *446*, 1023–1029.
- (46) Raman, R.; Venkataraman, M.; Ramakrishnan, S.; Lang, W.; Raguram, S.; Sasisekharan, R. *Glycobiology* **2006**, *16*, 82R–90R.
- (47) Mùthing, J.; Duvar, S.; Heitmann, D.; Hanisch, F.-G.; Neumann, U.; Lochnit, G.; Geyer, R.; Peter-Katalinić, J. *Glycobiology* **1999**, *9*, 459–468.

Table 1. Common Mammalian Neutral GSLs and Ganglioside Core Structures^a

GSL	structure	symbol
Lc2Cer	Gal β 4Glc β 1Cer	Lc2
globo series		
Gb3Cer	Gal α 4Gal β 4Glc β 1Cer	Gb3
Gb4Cer	GalNAc β 3Gal α 4Gal β 4Glc β 1Cer	Gb4
ganglio series		
Gg3Cer	GalNAc β 4Gal β 4Glc β 1Cer	Gg3
Gg4Cer	Gal β 3GalNAc β 4Gal β 4Glc β 1Cer	Gg4
neolacto series		
nLc4Cer	Gal β 4GlcNAc β 3Gal β 4Glc β 1Cer	nLc4
nLc6Cer	(Gal β 4GlcNAc β 3) $_2$ Gal β 4Glc β 1Cer	nLc6
nLc8Cer	(Gal β 4GlcNAc β 3) $_3$ Gal β 4Glc β 1Cer	nLc8

^a According to the 1997 IUPAC-IUBM recommendations.⁴⁴

Collection (Rockville, MD). The preparation and specificities of chicken polyclonal AB2-3 and AB2-6 antibodies, which recognize the iso-CD75s-gangliosides IV³Neu5Ac-nLc4Cer and VI³Neu5Ac-nLc6Cer with Neu5Ac α 3Gal β 4GlcNAc terminus and the CD75s-gangliosides IV⁶Neu5Ac-nLc4Cer and VI⁶Neu5Ac-nLc6Cer with Neu5Ac α 6Gal β 4GlcNAc residue, respectively, have been previously described.^{15,48}

Toxins and Antitoxin Antibodies. Cholera toxin B subunit (CTB) specific for ganglioside GM1 was from Sigma (No. C-7771; Taufkirchen, Germany) and goat anti-CTB antiserum from Calbiochem (No. 227040; Frankfurt a.M., Germany). Shiga toxin 1 (Stx1) was produced and purified as described.⁴⁰ The monoclonal mouse IgG anti-Stx1 antibody 109/4-E9b was from Sifin (Berlin, Germany). *Ricinus communis* lectin (RCL) was a kind gift of Dr. F. Stirpe (University of Bologna, Italy). Polyclonal rabbit anti-RCL antibody was purchased from Sigma (No. R-1254). CTB, Stx1, and RCL are highly potent toxins when reaching the body via the parenteral route (intravenous, subcutaneous, and intramuscular), whereas the enteral route (oral) toxicity is relatively low. Thus, handling of the toxins should be done with utmost care, using gloves and avoiding highly concentrated working dilutions and sharp or pointed tools.

Surgical Specimens. Tissue samples of hepatocellular carcinomas (patients 1 and 2) and pancreatic tumors (patients 3 and 4) were taken from patients that had undergone surgery for their primary tumors under an approved protocol of the local ethic committee.¹⁵ Tumor specimens were snap frozen in liquid nitrogen immediately after removal and stored at -80 °C until use. Corresponding control specimens were obtained from the same patient at organ sites without macroscopic tumor involvement and a minimal distance to the tumor of 5 (liver) and 2 cm (pancreas). Tissue wet weights of normal and cancerous tissues, respectively, were 46.1 and 263.7 mg (patient 1), 49.5 and 72.2 mg (patient 2), 13.8 and 45.2 mg (patient 3), and 197.5 and 75.8 mg (patient 4).

Preparation of Lipid Extracts from Surgical Specimens. Tissues were homogenized and extracted each with 4 mL of chloroform/methanol (1/2, v/v), 4 mL of chloroform/methanol (1/1, v/v), and 4 mL of chloroform/methanol (2/1, v/v). The combined supernatants of each tissue sample (12 mL) were dried

by rotary evaporation, and phospholipids were saponified by incubation with 4 mL of aqueous 1 N NaOH for 1 h at 37 °C. After neutralization with 400 μ L of 10 N HCl, the samples were dialyzed against deionized water and dried by rotary evaporation. The extracts were adjusted to defined volumes of chloroform/methanol (2/1, v/v) corresponding to 0.1 mg wet weight/ μ L.

High-Performance Thin-Layer Chromatography. GSLs were applied to glass-backed silica gel 60 precoated high-performance thin-layer chromatography plates (HPTLC plates, No. 5633; Merck, Darmstadt, Germany) with an automatic applicator (Linomat IV, CAMAG, Muttenz, Switzerland). Neutral GSLs were separated in solvent 1 composed of chloroform/methanol/water (120/70/17, each by volume) and gangliosides in solvent 2 consisting of chloroform/methanol/water (120/85/20, each by volume), both supplemented with 2 mM CaCl₂. Neutral GSLs and gangliosides were visualized with orcinol. Pinkish violet orcinol stained and deep blue colored overlay assay detected immunostained GSL bands (see TLC Overlay Assay) were quantified with a CD60 scanner (Desaga, Heidelberg, Germany, software ProQuant[®], version 1.06.000). Bands were scanned in reflectance mode at 544 (orcinol) and 630 nm (indolyphosphate) with a light beam slit of 0.02 mm \times 3 mm. The amounts of single neolacto series neutral GSLs and gangliosides (see Reference GSLs) were determined in orcinol-stained chromatograms of reference mixtures from human granulocytes with well-known total GSL content. Mixtures of 10 μ g of neutral GSLs contained 0.65 and 0.85 μ g of nLc4Cer (d18:1, C24:1/C24:0) and nLc4Cer (d18:1, C16:0), respectively, and 0.12 and 0.15 μ g of nLc6Cer (d18:1, C24:1/C24:0) and nLc6Cer (d18:1, C16:0), respectively. The amounts of 0.80 and 0.39 μ g of IV³Neu5Ac-nLc4Cer (d18:1, C24:1/C24:0) and IV³Neu5Ac-nLc4Cer (d18:1, C16:0), respectively, and 1.95 and 1.13 μ g of IV⁶Neu5Ac-nLc4Cer (d18:1, C24:1) and IV⁶Neu5Ac-nLc4Cer (d18:1, C16:0), respectively, were detected in 10 μ g of the ganglioside mixture. Serial dilutions of these well-defined standard mixtures were separated by TLC and used to determine the detection limits of individual GSLs employing antibodies (see TLC Overlay Assay) in combination with mass spectrometry (see Direct TLC-IR-MALDI-o-TOF-MS Analysis).

TLC Overlay Assay. GSLs were separated in two parallel runs. One of the parallel runs was stained with orcinol and the other used for the corresponding overlay assay. The TLC immunodetection procedure using anti-GSL antibodies and toxins in conjunction with antitoxin antibodies was employed as previously described.^{40,42,47,48} Anti-GSL antibodies, toxins, antitoxin, and secondary anti-Ig subtype antibodies were diluted with 1% (w/v) bovine serum albumin in phosphate-buffered saline (solution A). Briefly, polyclonal chicken anti-Gal β 4GlcNAc-R, AB2-3, and AB2-6 antibodies were used in 1:2000 dilution. The supernatant from hybridoma TIB 189, producing the monoclonal mouse IgM anti-Gal β 4GlcNAc-R antibody 1B2-1B7, was used 1:10 diluted.

Stx1 (0.2 μ g/mL) was detected with the anti-Stx1 monoclonal antibody 109/4-E9b (2 μ g/mL),⁴⁰ CTB (0.25 μ g/mL) with the polyclonal goat anti-CTB antibody (1:4000),⁴¹ and RCL (1 μ g/mL) with the polyclonal rabbit anti-RCL antibody (1:200).⁴² All secondary antibodies, namely, goat anti-mouse IgG plus IgM, goat anti-rabbit IgG, rabbit anti-chicken IgY, and rabbit anti-goat IgG (all from Dianova, Hamburg, Germany) were used in 1:2000 dilutions. Bound secondary antibodies were visualized with 0.05% (w/v)

(48) Meisen, I.; Peter-Katalinić, J.; Müthing, J. *Anal. Chem.* **2003**, *75*, 5719–5725.

5-bromo-4-chloro-3-indolylphosphate p-toluidine salt (BCIP; No. 6368.3; Roth, Karlsruhe, Germany) in glycine buffer (0.1 M glycine, 1 mM ZnCl₂, 1 mM MgCl₂, pH 10.4). The immunostained chromatograms were washed with glycine buffer and stored at -20 °C.

Infrared Matrix-Assisted Laser Desorption/Ionization Orthogonal Time-of-Flight Mass Spectrometer. The specifications of the IR-MALDI-o-TOF mass spectrometer (MDS Sciex, Concord, ON, Canada), which routinely provides a mass resolution of ~10 000 and a mass accuracy of ~20 ppm, have been described in detail in three recent publications.^{37–39} The mass spectrometer is equipped with an Er:YAG laser (Bioscope, BiOptics Laser Systems AG, Berlin, Germany), emitting pulses of ~100 ns duration at a wavelength of 2.94 μm. This wavelength coincides well with vibrational modes of the OH groups of the glycerol MALDI matrix. The IR radiation is coupled into the ion source and the laser beam directed onto the target yielding a focal spot size of ~250 μm in diameter. Samples can be observed with a CCD camera with 10-μm optical resolution. For analysis in the positive ion mode, the TOF pusher was operated at 10 kV. Mass spectra were processed and evaluated with the MoverZ3 software (version 2002.02.20, Genomics Solutions, Ann Arbor, MI).

Our instrument is a prototype of the commercial pOTOF 2000 from Perkin-Elmer. Similar o-TOF instruments are, for example, the ABI Qstar and the Waters QTOF Premier. All have in common that the ion source is filled with N₂ background gas of ~1 mbar. This decouples the desorption/ionization process from the mass determination in the high-vacuum TOF-MS part. Electrical quadrupoles guide the ions through the differential pressure regions. This way, the accurate mass analysis from even very rough and electrically nonconducting surfaces becomes possible without loss in performance—a major advantage in the analysis from the TLC plates.

Direct TLC-IR-MALDI-o-TOF-MS Analysis. Direct TLC-IR-MALDI-o-TOF-MS analysis was performed in situ from immunopositive bands (see TLC Overlay Assay). The immunostained TLC plates were soaked for 2 h in 10 mM ammonium acetate buffer (pH 3.6) and dried at room temperature. The silica gel fixative (Plexigum P28, Röhm, Darmstadt, Germany), which is generally used to prevent peeling off the silica gel from the glass support, was removed by three consecutive dippings in distilled chloroform. For MS analysis, the TLC plates were cut to pieces of ~15 mm × 40 mm and fixed on the sample probe with double-sided adhesive pads. Droplets of ~0.3 μL of the glycerol matrix were then applied with a pipet across the immunopositive bands. The glycerol was soaked up by the silica gel and spread out to wetted spots of ~2 mm in diameter. For acquisition of the spectra, 100–300 single laser pulses were typically applied on different random positions within the ~2-mm-wide TLC-immunostained bands. GSLs were analyzed in the positive ion mode.

RESULTS

General Strategy of Direct TLC-IR-MALDI-MS Analysis.

The schematic representation of in situ IR-MALDI-MS of immunostained GSLs is shown in Figure 1a. GSL mixtures are separated by high-performance TLC on a silica gel-coated TLC plate. After plastic fixation of the silica gel, the chromatogram is consecutively overlaid with the primary anti-GSL and secondary alkaline phosphatase-labeled antibodies. Bound antibodies are detected by blue

BCIP-derived precipitates. The fixative is then removed by chloroform extraction, the TLC plate cut into appropriate pieces for insertion into the ion source, and the glycerol matrix added to the immunostained bands. Desorption/ionization of GSLs by the focused IR laser beam is achieved directly from the immunostained bands resulting in the MALDI mass spectrum.

TLC Immunodetection of Neutral GSLs. As shown by the orcinol stain in Figure 1b, major neutral GSLs from human granulocytes are Lc2Cer (bands 1 and 2) and neolacto series nLc4Cer (bands 3 and 4) accompanied by minor nLc6Cer (bands 5 and 6) and nLc8Cer (bands 7 and 8), the elongation products of nLc4Cer by one and two Galβ4GlcNAc repeats, respectively (for structures see Table 1). Based on the different substitution of the sphingosine (d18:1) moiety of each GSL with a fatty acid of varying alkyl chain length, neutral GSLs carrying two (Lc2Cer) to eight sugars (nLc8Cer) separate in double bands, whereby the upper band represents the GSL species with the long chain and the lower band that with the short-chain fatty acid (determined in detail by MS analysis further down). In the development of the TLC-IR-MALDI-MS strategy, we initially performed two TLC overlays with these neutral GSLs of well-known structures using a polyclonal chicken IgY (pAb) and a monoclonal mouse IgM (mAb) antibody, both directed to the Galβ4GlcNAc epitope (Figure 1b). The pAb preferentially binds to nLc4Cer and nLc6Cer and to a minor extent to Lc2Cer (slight cross-reactivity with the Galβ4Glc epitope). The mAb exhibited a pronounced binding to nLc6Cer and nLc8Cer beside its binding to nLc4Cer.

Direct TLC-IR-MALDI-MS of Immunodetected Neutral GSLs. As a proof of concept, the antibody stained bands were analyzed by in situ IR-MALDI-MS. All neutral GSL species primarily appear as monosodiated [M + Na]⁺ molecular ions in the positive ion mode mass spectra, accompanied by minor corresponding disodiated [M + 2Na - H]⁺ molecular ions. This is shown for pAb and mAb immunostained nLc4Cer of band 4 in Figure 1c and 1d, respectively and for pAb and mAb immunostained nLc6Cer of band 6 in Figure 1e and f, respectively. The pAb positive nLc4Cer of band 4 (Figure 1c) is detected as monosodiated ion at *m/z* 1249.72 and with lower abundance as disodiated ion at *m/z* 1271.70 confirming the structure as nLc4Cer (d18:1, C16:0). The same results were obtained for mAb immunostained nLc4Cer of band 4 (Figure 1d). The mass spectra of pAb and mAb immunostained nLc4Cer of band 3, identified as nLc4Cer (d18:1, C24:1/C24:0), are displayed in Figure S-1a and S-1b, respectively, of the Supporting Information. The pAb positive nLc6Cer of band 6 (Figure 1e) is detected as monosodiated ion at *m/z* 1614.85 and with lower abundance as disodiated ion at *m/z* 1636.83 confirming the structure as nLc6Cer (d18:1, C16:0). Similar results were obtained for mAb immunostained nLc6Cer of band 6 (Figure 1f). The mass spectra of pAb and mAb immunostained nLc6Cer of band 5, identified as nLc6Cer (d18:1, C24:1/C24:0), are displayed in Figure S-1c and S-1d, respectively, of the Supporting Information. Molecular ions and structures of the TLC-IR-MALDI detected GSLs are listed in Table S-1 of the Supporting Information. Thus, when comparing the mass spectra, in principle the same high mass accuracy was achieved independent of type and size of the employed antibodies (IgY 150 kDa; IgM 950 kDa). However, a somewhat enhanced sensitivity with respect to the signal intensities obtained from the pAb immun-

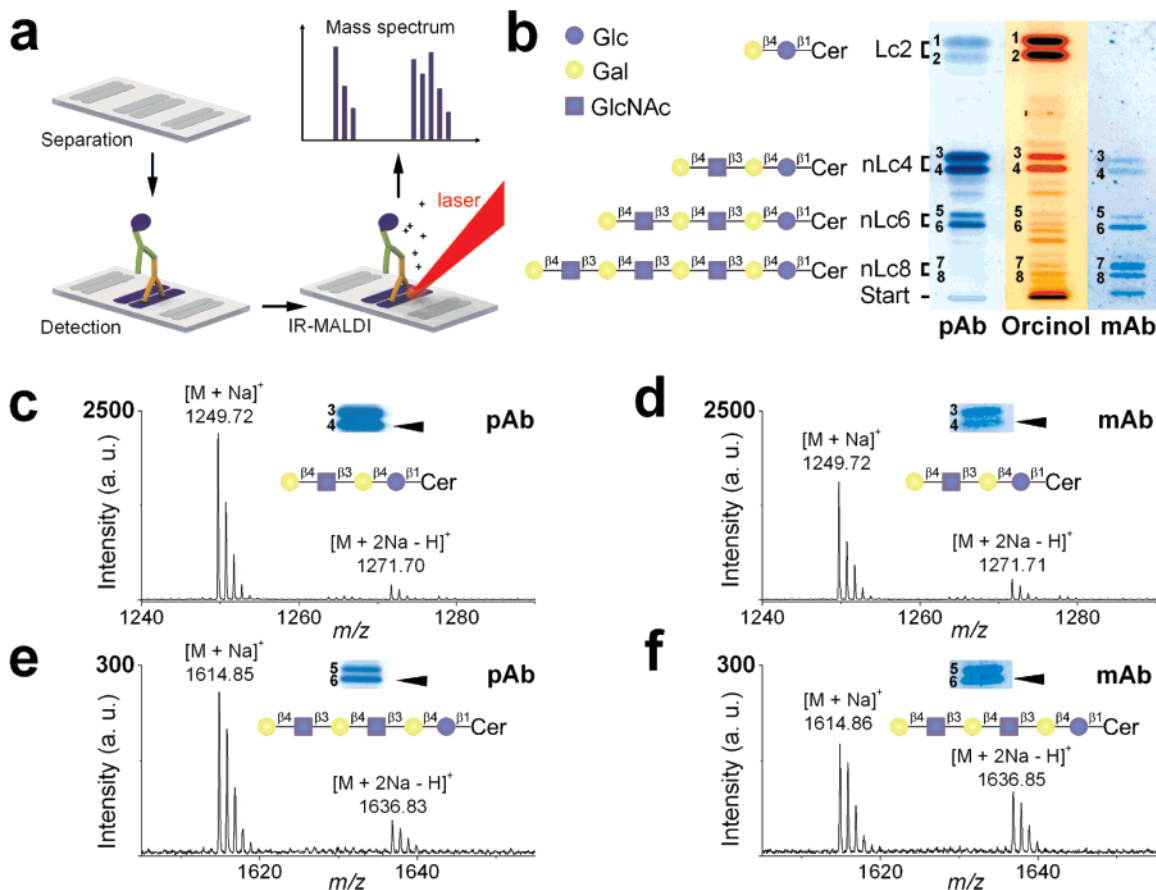


Figure 1. Direct TLC-IR-MALDI-MS of immunodetected GSLs. (a) Scheme of matching the TLC overlay assay with IR-MALDI-MS. (b) TLC immunostain of neutral GSLs with Gal β 4GlcNAc-specific polyclonal chicken IgY (pAb) and monoclonal mouse IgM antibody (mAb). Total amounts of 22.5 and 0.3 μ g of neutral GSLs from human granulocytes were separated and detected by orcinol and TLC immunostain, respectively. Symbols and abbreviations for each GSL (numbered from 1 to 8 from top to bottom) are indicated, and their structures are listed in Table 1. For direct TLC-IR-MALDI-MS, amounts of 3.0 μ g of total neutral GSLs were applied and mass spectra were acquired from 255 ng of pAb (c) and mAb (d) immunostained nLc4Cer (d18:1, C16:0) and from 45 ng of pAb (e) and mAb (f) immunostained nLc6Cer (d18:1, C16:0), all marked with arrowheads. Type of molecular ions, m/z values, and structures of GSLs are listed in Table S-1 of the Supporting Information.

obtained neutral GSL bands is obvious in comparison to the signal intensities obtained from the mAb immunostained bands (Figure 1 and Figure S-1). The most plausible but speculative reason is that the size of the anti-GSL antibody (small IgY versus large IgM) might influence the ionization of the bound GSLs.

Limits of Detection. In order to determine TLC-IR-MALDI-MS detection limits, serial dilutions of the TLC-separated reference GSL mixture were analyzed. Approximate MS limits for pAb detected nLc4Cer (d18:1, C24:1/C24:0) and nLc4Cer (d18:1, C16:0) were obtained at the amounts of 1.9 and 0.6 ng, respectively, as shown in Figure 2a, and for the corresponding mAb detected nLc4Cer species at 9.7 and 6.4 ng, respectively (Figure 2b). The limits of MS detection of pAb and mAb immunostained nLc6Cer were on the same order of magnitude and are displayed in Figure S-2a and S-2b, respectively, of the Supporting Information. As a rule of thumb, combined TLC-immunodetection and IR-MALDI-MS operate at nanogram quantities of single neutral GSLs, showing as general trends (i) slightly enhanced sensitivity of pAb-detected GSLs and (ii) little higher sensitivity of both types of antibodies for GSLs carrying short-chain fatty acids.

TLC Immunodetection of Gangliosides. Next, the suitability of immunolabeled gangliosides for the structural analysis by TLC-IR-MALDI-MS was investigated. A mixture of well-known gan-

gliosides from human granulocytes, which contains the gangliosides GM3 and isomers of terminally α 2-6- and α 2-3-sialylated nLc4Cer and extended nLc6Cer core structures, was used. CD75s-gangliosides with Neu5Ac α 6Gal β 4GlcNAc terminus, detectable with the AB2-6 antibody,⁴⁸ were IV⁶Neu5Ac-nLc4Cer and core-extended VI⁶Neu5Ac-nLc6Cer. The iso-CD75s-gangliosides with Neu5Ac α 3Gal β 4GlcNAc terminus, detectable with the AB2-3 antibody,⁴⁸ were IV³Neu5Ac-nLc4Cer and core-extended VI³Neu5Ac-nLc6Cer. As shown in the orcinol stain of Figure 3a, CD75s- and iso-CD75s-gangliosides chromatograph as double bands on TLC plates due to fatty acid variability in the ceramide part along the lines of the neutral GSLs as described above. The AB2-6 antibody specifically binds to IV⁶Neu5Ac-nLc4Cer and VI⁶Neu5Ac-nLc6Cer but not to their isomeric counterparts IV³Neu5Ac-nLc4Cer and VI³Neu5Ac-nLc6Cer (Figure 3a).

Direct TLC-IR-MALDI-MS of Immunodetected Gangliosides. *CD75s-Gangliosides.* The AB2-6 antibody binds to the CD75s-gangliosides IV⁶Neu5Ac-nLc4Cer of bands 5 and 6 and VI⁶Neu5Ac-nLc6Cer of bands 9 and 10 (Figure 3a). The mass spectra of AB2-6 immunostained IV⁶Neu5Ac-nLc4Cer of bands 5 and 6 are displayed in Figure 3b and c, and those of AB2-6 immunostained VI⁶Neu5Ac-nLc6Cer of bands 9 and 10 in Figure 3d and e, respectively. On principle, all monosialylated gangliosides

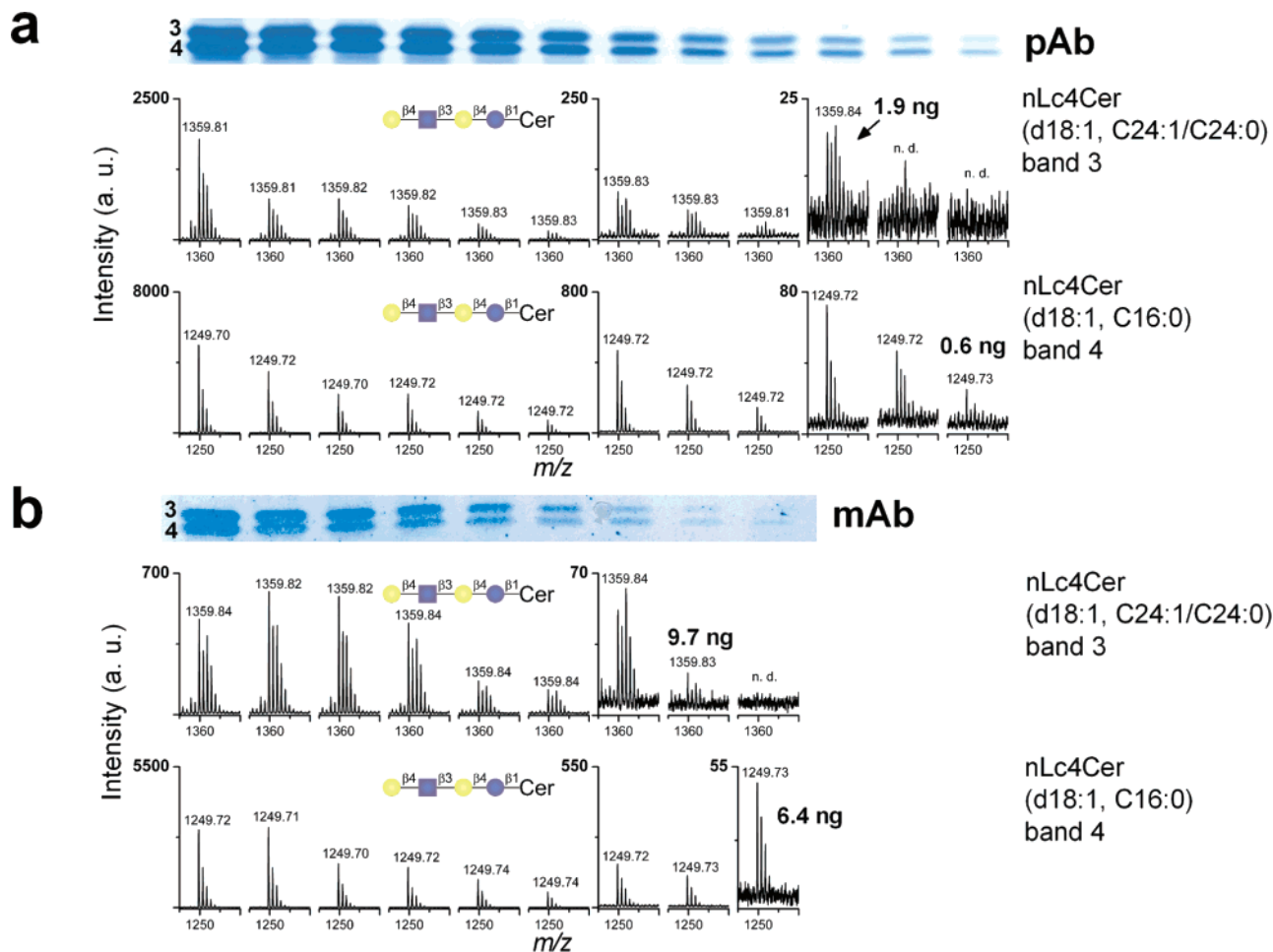


Figure 2. TLC-IR-MALDI-MS detection limits of pAb and mAb immunostained nLc4Cer. Decreasing amounts from 30 to 7.5 ng of the total neutral GSL mixture of human granulocytes. They were separated and the immunostain of Gal β 4GlcNAc-terminated GSLs was performed as described in Figure 1. The cutout of the immunostained chromatogram shows the decreasing amounts of immunolabeled nLc4Cer from the left to the right and the approximate MS detection limits of the single nLc4Cer species as indicated. (a) Detection limits of pAb immunostained nLc4Cer (d18:1, C24:1/C24:0) of band 3 and nLc4Cer (d18:1, C16:0) of band 4. (b) Detection limits of mAb immunostained nLc4Cer (d18:1, C24:1/C24:0) of band 3 and nLc4Cer (d18:1, C16:0) of band 4.

preferentially appear as doubly sodiated $[M_2 + 2Na - H]^+$ molecular ions in the positive ion mode mass spectra accompanied by corresponding but minor monosodiated $[M_2 + Na]^+$ molecular ions and less intensive $[M_1 + Na]^+$ ions of desialylated gangliosides. The latter appear, as expected from the neutral GSL spectra, predominantly as monosodiated molecular ions and indicate a low degree of fragmentation due to the loss of terminal sialic acid.

The major species detected from band 5 (Figure 3b) corresponds to doubly sodiated IV⁶Neu5Ac-nLc4Cer molecules with C24:1 fatty acids (m/z 1672.89) and the minor species to the monosodiated counterpart (m/z 1650.91) and the desialylated mother ion (m/z 1359.81). The molecular ions obtained from band 6 (Figure 3c) revealed doubly sodiated IV⁶Neu5Ac-nLc4Cer with C16:0 fatty acids (m/z 1562.79) as the predominant molecular ion accompanied by its minor monosodiated counterpart (m/z 1540.81) and the desialylated precursor ion (m/z 1249.72). The molecular ions acquired from the α 2-6-sialylated nLc6Cer core gangliosides exhibited the same principal features as the α 2-6-sialylated nLc4Cer core gangliosides. Disodiated molecular ions of gangliosides VI⁶Neu5Ac-nLc6Cer (d18:1, C24:1) and VI⁶Neu5Ac-nLc6Cer (d18:1, C16:0) form the base peaks at m/z 2038.04 and 1927.91, respectively, as shown in Figure 3d and e. Both ganglioside

species were flanked by their corresponding monosodiated molecular ions and desialylated precursor ions. All AB2-6 immunostained and IR-MALDI detected gangliosides are listed in Table S-2 of the Supporting Information. The approximate MS detection limits for IV⁶Neu5Ac-nLc4Cer (d18:1, C24:1) were determined at 5.9 ng and for IV⁶Neu5Ac-nLc4Cer (d18:1, C16:0) at 3.4 ng, respectively as demonstrated in Figure S-3a and S-3b of the Supporting Information.

Iso-CD75s-gangliosides. An analogous series of TLC-IR-MALDI-MS analyses of terminally α 2-3-sialylated gangliosides IV³-Neu5Ac-nLc4Cer (bands 3 and 4) and VI³Neu5Ac-nLc6Cer (bands 7 and 8) was performed (see orcinol stain in Figure 3a). These gangliosides were detected with the AB2-3 antibody,⁴⁸ which specifically binds to the Neu5Ac α 3Gal β 4GlcNAc epitope. The pattern of the molecular ions in the mass spectra of AB2-3 antibody stained iso-CD75s-gangliosides was similar to those obtained with the AB2-6 detected CD75s-gangliosides, and the data are provided in Figure S-4 of the Supporting Information. A remarkable difference was the presence of C24:0 fatty acids in addition to C24:1 fatty acids in α 2-3-sialylated gangliosides. All AB2-3 immunostained and IR-MALDI detected gangliosides are listed in Table S-2 of the Supporting Information. The approximate MS

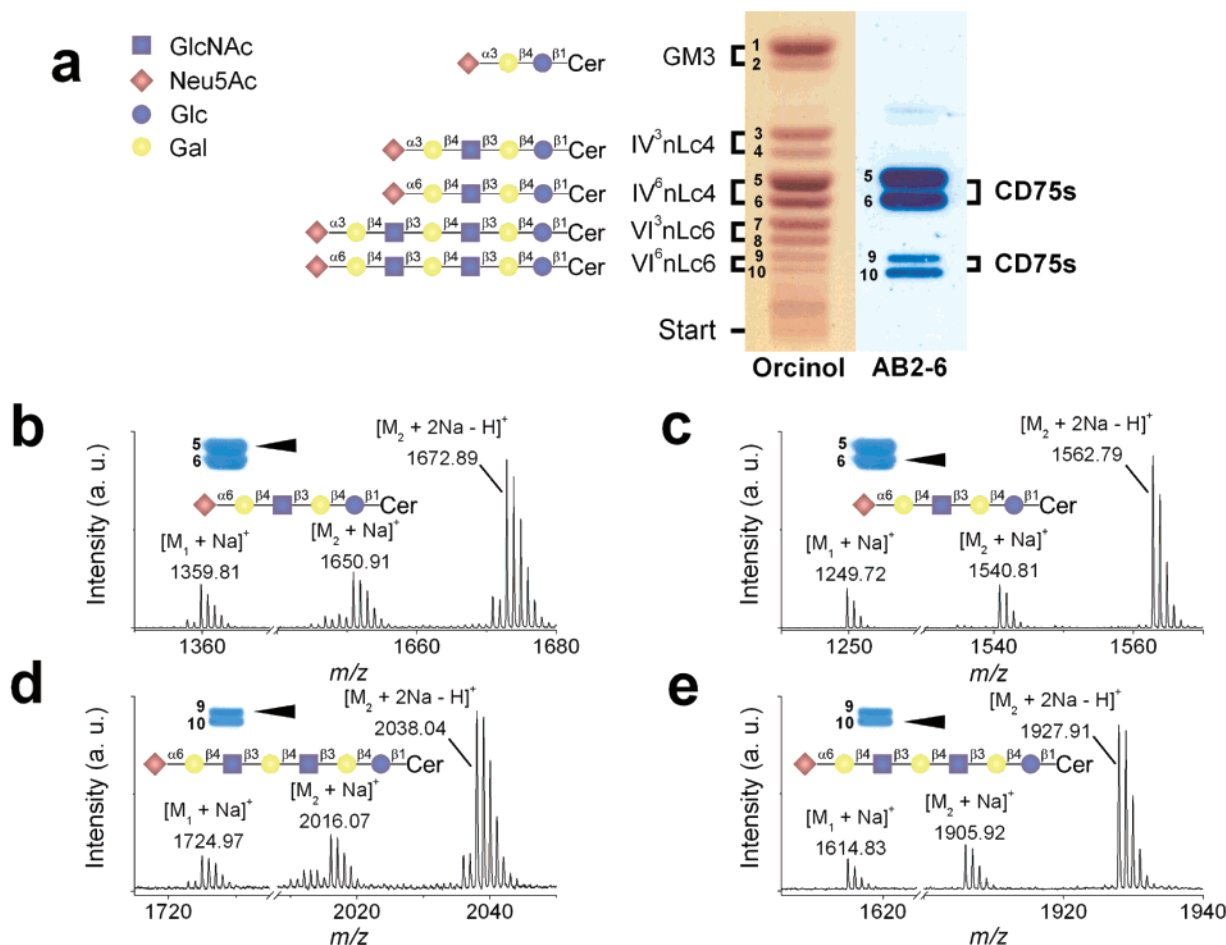


Figure 3. Direct TLC-IR-MALDI-MS of immunostained CD75s-gangliosides with Neu5Ac α 6Gal β 4GlcNAc-terminus. (a) TLC immunostain of IV⁶Neu5Ac-nLc4Cer and core-extended VI⁶Neu5Ac-nLc6Cer with polyclonal antibody AB2-6. Total amounts of 7.5 and 1.2 μ g of gangliosides were separated and detected by sugar staining (orcinol) and TLC immunostain, respectively. Symbols and abbreviations for each ganglioside (numbered from 1 to 10 from top to bottom) are indicated, and their core structures are listed in Table 1. For direct TLC-IR-MALDI-MS, amounts of 7.5 μ g of total gangliosides were separated and mass spectra were acquired from 1.46 μ g of IV⁶Neu5Ac-nLc4Cer (d18:1, C24:1) of band 5 (b), 0.85 μ g of IV⁶Neu5Ac-nLc4Cer (d18:1, C16:0) of band 6 (c), 0.26 μ g of VI⁶Neu5Ac-nLc6Cer (d18:1, C24:1) of band 9 (d), and 0.15 μ g of VI⁶Neu5Ac-nLc6Cer (d18:1, C16:0) of band 10 (e), all marked with arrowheads. Dominant $[M_2 + 2Na - H]^+$ and minor $[M_2 + Na]^+$ ions in the spectra represent the gangliosides and the less intensive $[M_1 + Na]^+$ ions the corresponding desialylated gangliosides. Type of molecular ions, m/z values, and structures of gangliosides are listed in Table S-2 of the Supporting Information.

detection limits for IV³Neu5Ac-nLc4Cer carrying long and short-chain fatty acids were determined at 6.0 and 1.2 ng (bands 3 and 4), respectively (data not shown).

Thus, combined TLC-immunodetection and IR-MALDI-MS work absolutely reliably on a nanogram scale of single gangliosides with a somewhat enhanced sensitivity for gangliosides carrying short-chain fatty acids.

Direct TLC-IR-MALDI-MS of Bacterial Toxin and Plant Lectin Binding GSLs. The appropriateness of various GSL binding bacterial toxins and a plant lectin for TLC-IR-MALDI-MS was examined by employing reference mixtures of well-known neutral GSLs or gangliosides. Toxins produced by pathogenic bacteria, namely, the CTB of *Vibrio cholerae* and Stx1 from enterohemorrhagic *Escherichia coli*, were chosen. The highly toxic *R. communis* lectin (RCL) was used as a representative plant derived ribosome inactivating protein.

The CTB specifically binds to the ganglio series ganglioside GM1⁴⁹ as shown by the TLC overlay assay in the inset of Figure

4a. A ganglioside mixture from human brain was separated and GM1 detected by CTB/anti-CTB immunostain. The mass spectrum yields two major disodiated molecular ions which can be clearly distinguished as GM1 (d18:1, C18:0) with m/z 1590.83 $[M_1 + 2Na - H]^+$ and GM1 (d18:1, C20:0) with m/z 1618.87 $[M_2 + 2Na - H]^+$. The molecular ions at m/z 1568.85 $[M_1 + Na]^+$ and 1596.88 $[M_2 + Na]^+$ indicate the monosodiated species in line with C18:0 and C20:0 fatty acid carrying GM1, respectively.

The neutral GSL Gb3Cer (CD77) is the preferential receptor of the pentameric B subunit of Stx1.⁵⁰ In order to structurally characterize Stx1 binding Gb3Cer species, a neutral GSL mixture of human erythrocytes, known to contain considerable quantities of high- and low-affinity binding Stx1 ligands Gb3Cer and Gb4Cer, respectively,⁴⁰ was chromatographed and the Stx1/anti-Stx1 immunostained Gb3Cer bands were applied to IR-MALDI-MS (Figure 4b and c). The $[M_2 + Na]^+$ ions from the upper Stx1 positive TLC band with the highest signal intensities at m/z 1156.79/1158.81 in the mass spectrum of Figure 4b corresponds

(49) Fishman, P. H. *J. Membr. Biol.* **1982**, *69*, 85–97.

(50) Lingwood, C. A. *Trends Microbiol.* **1996**, *4*, 147–153.

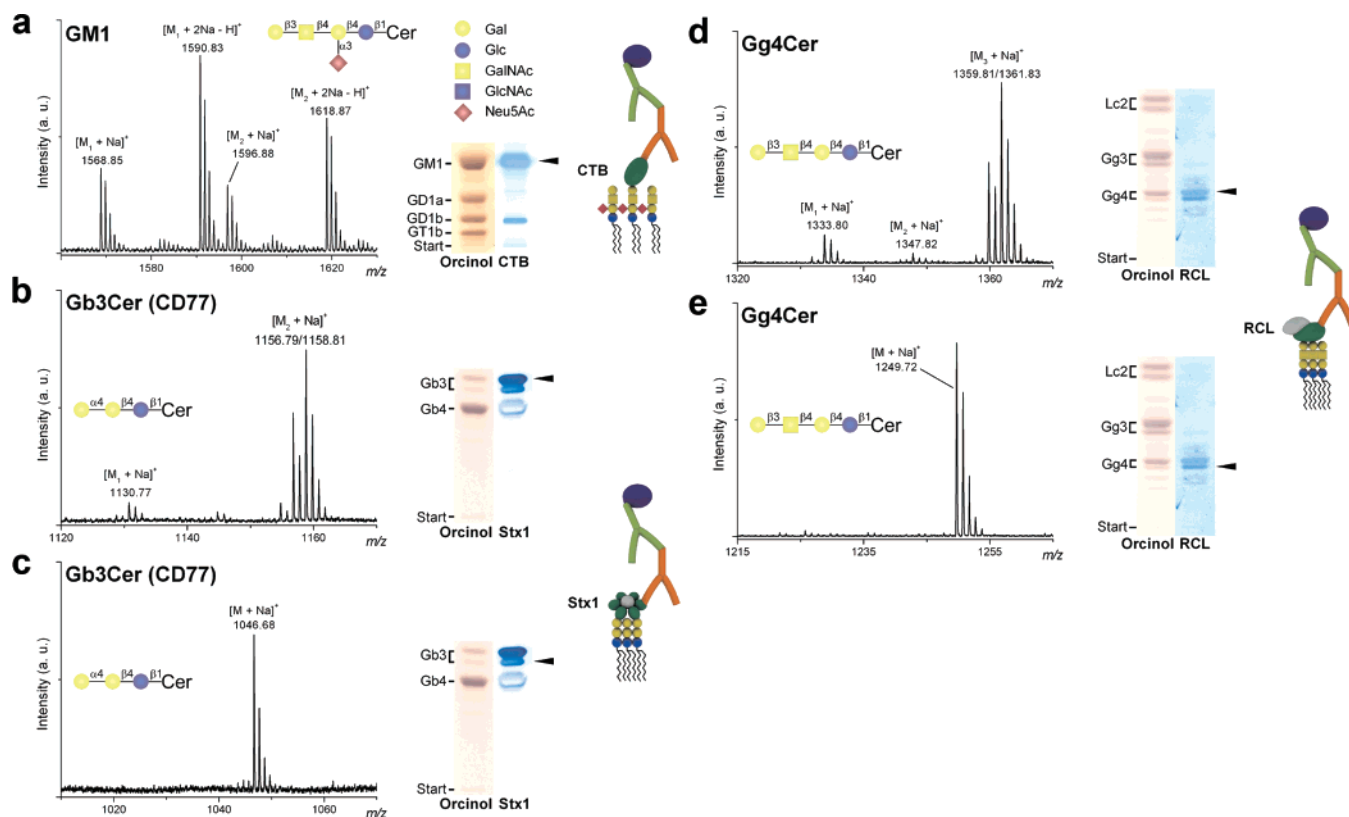


Figure 4. Direct TLC-IR-MALDI-MS of GSLs detected with bacterial toxins and a plant lectin. GSLs were chromatographed and detected by orcinol staining and overlaying the TLC plate with toxin or lectin followed by immunostain. GSL species analyzed by MS are marked with arrowheads in each panel. The schemes in the right-hand sides of the panels illustrate the different principles in the detection of GSLs. (a) CTB. Total amounts of 20 and 2 μg of human brain gangliosides were applied for the orcinol and the CTB overlay assay, respectively. The dominant $[\text{M}_1 + 2\text{Na} - \text{H}]^+$ and $[\text{M}_2 + 2\text{Na} - \text{H}]^+$ ions could be assigned to GM1 (d18:1, C18:0) and GM1 (d18:1, C20:0), respectively, flanked by their corresponding less abundant $[\text{M}_1 + \text{Na}]^+$ and $[\text{M}_2 + \text{Na}]^+$ ions. (b, c) AB₅ Shiga toxin (Stx) 1. Total amounts of 10 μg of neutral GSLs from human erythrocytes were applied for the orcinol and the Stx1 overlay assay. In the upper Stx1-positive band (b), the prevalent $[\text{M}_2 + \text{Na}]^+$ ions are indicative for Gb3Cer (d18:1, C24:1/C24:0) and the minor $[\text{M}_1 + \text{Na}]^+$ ions for Gb3Cer (d18:1, C22:0). The lower Stx1-positive band (c) contains Gb3Cer (d18:1, C24:0) evidenced by the $[\text{M} + \text{Na}]^+$ ions. (d, e) Dimeric *R. communis* lectin (RCL). Total amounts of 16 μg of neutral GSLs from mouse lymphoma cell line MDAY-D2 were applied for the orcinol and the RCL overlay assay. In the upper RCL-positive band (d), the predominant $[\text{M}_3 + \text{Na}]^+$ ions correspond to Gg4Cer (d18:1, C24:1/C24:0) accompanied by minor $[\text{M}_2 + \text{Na}]^+$ and $[\text{M}_1 + \text{Na}]^+$ ions representing Gg4Cer (d18:1, C23:0) and Gg4Cer (d18:1, C22:0), respectively. The lower RCL-positive band (e) contains Gg4Cer (d18:1, C16:0) evidenced by the $[\text{M} + \text{Na}]^+$ ions. Type of molecular ions, m/z values, and structures of GSLs are listed in Table S-3 of the Supporting Information.

to Gb3Cer (d18:1, C24:1/C24:0) as the prevalent Stx1 ligands in the GSL mixture, flanked by minor $[\text{M}_1 + \text{Na}]^+$ ions of Gb3Cer (d18:1, C22:0) at m/z 1130.77. Deduced from the Stx1 overlay assay and the IR-MALDI-MS analysis, the $[\text{M} + \text{Na}]^+$ ions at m/z 1046.68 were assigned to the lower Stx1 binding Gb3Cer (d18:1, C16:0) species (Figure 4c).

Ganglio series neutral GSLs with Gal β GalNAc terminus are appropriate binding ligands for the B subunit of the galactose-specific RCL.⁴² A mixture of neutral GSLs, which comprises gangliotetraosylceramide (Gg4Cer) as one of the dominant constituents, was used for the RCL/anti-RCL overlay assay. IR-MALDI-MS of the upper and lower RCL positive GSL band are depicted in Figure 4d and e, respectively. The $[\text{M}_3 + \text{Na}]^+$ ions recorded at m/z 1359.81/1361.83 were assigned to Gg4Cer (d18:1, C24:1/C24:0) and the low abundant $[\text{M}_2 + \text{Na}]^+$ and $[\text{M}_1 + \text{Na}]^+$ ions at m/z 1347.82 and 1333.80 to minor Gg4Cer variants with C23:0 and C22:0 fatty acids, respectively, as shown in Figure 4d. Regarding the lower RCL positive band in Figure 4e, the structural assignment of the $[\text{M} + \text{Na}]^+$ ions at m/z 1249.72 aimed at the identification of Gg4Cer (d18:1, C16:0). A synopsis of all

toxin and lectin detected GSLs is provided in Table S-3 of the Supporting Information.

The result of this comprehensive series of binding studies is that all carbohydrate-binding proteins so far investigated, namely, (i) CTB, (ii) AB₅ holotoxin (Stx1), and (iii) RCL, are appropriate candidates as probes for the structural characterization of their GSL receptors by TLC-IR-MALDI-MS.

Tracing Tumor-Associated GSLs in Crude Lipid Extracts.

In search of cancer-associated GSLs, i.e., GSLs showing enhanced expression in malignant compared to normal tissue, the idea was to avoid any laborious GSL isolation procedures with the objective to probe crude lipid extracts from small-sized tissue samples by TLC-IR-MALDI-MS. For that purpose, surgical specimens of human cancerous and unaffected tissue were extracted with organic solvents, coextracted phospholipids saponified by alkaline treatment and salts removed by dialysis as the single “purification” step. The general aptitude of such crude lipid extracts to TLC-IR-MALDI-MS analysis is exemplarily demonstrated for hepatocellular (patients 1 and 2) and pancreatic tumors (patients 3 and 4). Several tumor-associated GSLs were identified in the malignant

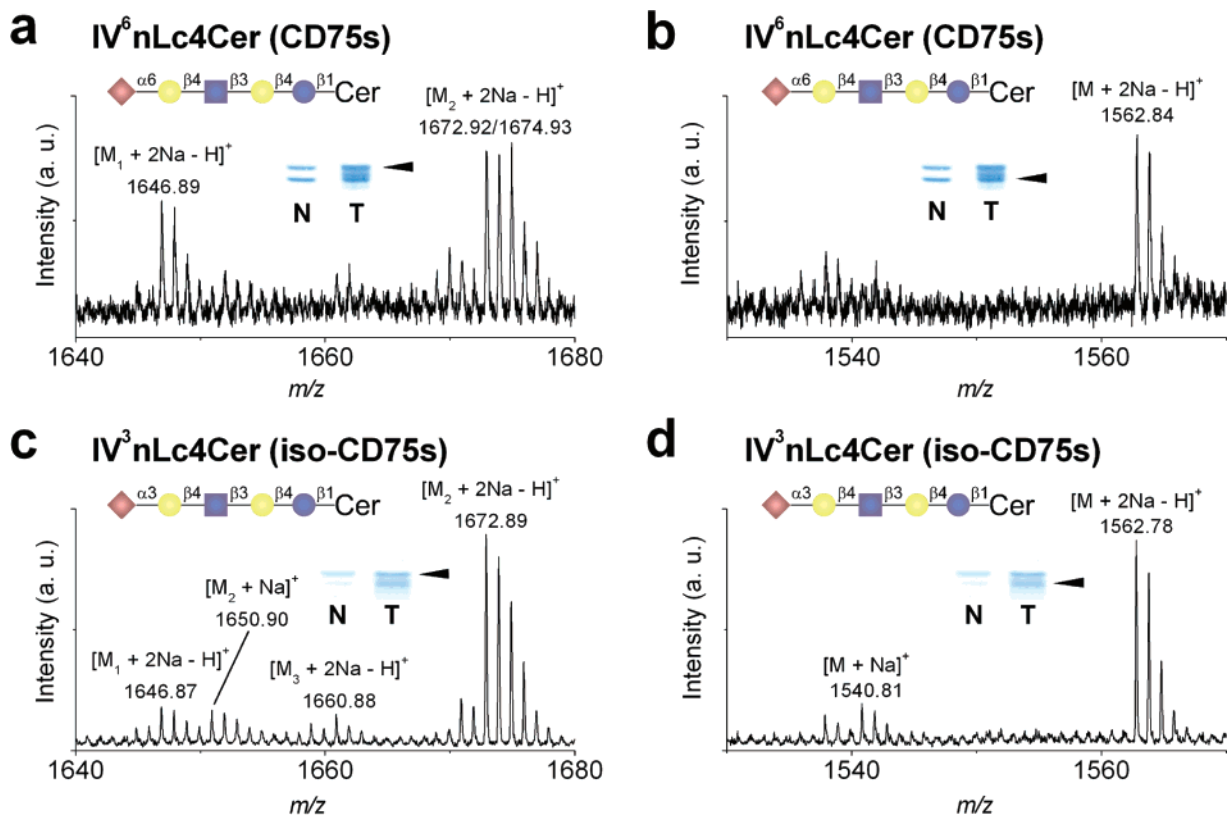


Figure 5. Tracing tumor-associated GSLs in hepatocellular cancer. Aliquots from crude lipid extracts of normal (N) and tumor tissue (T) were separated simultaneously by TLC, immunostained and the arrowhead marked tumor-associated GSLs analyzed by IR-MALDI-MS. (a, b) Patient 1. Extracts equivalent to 2 mg of wet weight tissue were applied and CD75s-gangliosides probed with antibody AB2-6. The $[M_2 + 2Na - H]^+$ and $[M_1 + 2Na - H]^+$ ions in panel a correspond to $IV^6Neu5Ac-nLc4Cer$ (d18:1, C24:1/C24:0) and $IV^6Neu5Ac-nLc4Cer$ (d18:1, C22:0), respectively, and the $[M + 2Na - H]^+$ ions in panel b to $IV^6Neu5Ac-nLc4Cer$ (d18:1, C16:0). (c, d) Patient 2. Extracts equivalent to 3 mg of wet weight tissue were applied and iso-CD75s-gangliosides probed with antibody AB2-3. Dominant $[M_2 + 2Na - H]^+$ and appropriate minor $[M_2 + Na]^+$ ions in panel c represent $IV^3Neu5Ac-nLc4Cer$ (d18:1, C24:1) and the less abundant $[M_1 + 2Na - H]^+$ and $[M_3 + 2Na - H]^+$ ions $IV^3Neu5Ac-nLc4Cer$ (d18:1, C22:0) and $IV^3Neu5Ac-nLc4Cer$ (d18:1, C23:0), respectively. The presence of $IV^3Neu5Ac-nLc4Cer$ (d18:1, C16:0) in panel d is evidenced by $[M + 2Na - H]^+$ and accompanying $[M + Na]^+$ ions. Type of molecular ions, m/z values, and proposed structures of GSLs are listed in Table S-5 of the Supporting Information. The basic histological characteristics of the tumors are summarized in Table S-4 of the Supporting Information.

tissues and their structures characterized according to their chromatographic behavior, antibody binding, and m/z values.

Probing Human Hepatocellular Carcinomas. The general applicability of TLC-IR-MALDI-MS using crude lipid extracts from the surgical specimens of patients 1 and 2 is shown in Figure 5. The direct comparison of TLC overlay assays employing the AB2-6 antibody for the normal (N) and the tumor sample (T) indicated an enhanced expression of CD75s-gangliosides in the tumor of patient 1. The $[M_2 + 2Na - H]^+$ and $[M_1 + 2Na - H]^+$ ions of the CD75s-positive upper band at m/z 1672.92/1674.93 and 1646.89 were assigned to the CD75s-gangliosides $IV^6Neu5Ac-nLc4Cer$ (d18:1, C24:1/C24:0) and $IV^6Neu5Ac-nLc4Cer$ (d18:1, C22:0), respectively (Figure 5a), and the $[M + 2Na - H]^+$ ions of the immunopositive lower band at m/z 1562.84 are indicative for $IV^6Neu5Ac-nLc4Cer$ (d18:1, C16:0) (Figure 5b).

In the malignant tissue sample of patient 2, a considerable increase of iso-CD75s-ganglioside $IV^3Neu5Ac-nLc4Cer$ (d18:1, C24:1), evidenced by $[M_2 + 2Na - H]^+$ ions at m/z 1672.89, was detected in the AB2-3 positive upper band (Figure 5c). This major ganglioside was accompanied by low abundant $IV^3Neu5Ac-nLc4Cer$ (d18:1, C22:0) and $IV^3Neu5Ac-nLc4Cer$ (d18:1, C23:0), indicated by the $[M_1 + 2Na - H]^+$ and $[M_3 + 2Na - H]^+$ ions at

m/z 1646.87 and 1660.88, respectively. The molecular ions of the immunolabeled lower band were allocated to the iso-CD75s-ganglioside $IV^3Neu5Ac-nLc4Cer$ (d18:1, C16:0) as shown in Figure 5d.

Probing Human Pancreas Carcinoma. Employing the anti-Gb3Cer antibody, a severely elevated expression of Gb3Cer variants was found in the cancerous tissue of patient 3 (Figure 6a and b). The dominant $[M_3 + Na]^+$ ions of the Gb3Cer positive upper band were assigned to Gb3Cer (d18:1, C24:1/C24:0) accompanied by minor Gb3Cer species carrying C22:0 $[M_1 + Na]^+$, C23:0 $[M_2 + Na]^+$, and C25:0 fatty acids $[M_4 + Na]^+$ (Figure 6a). In the antibody positive lower band Gb3Cer (d18:1, C16:0) is documented by the $[M + Na]^+$ ions at m/z 1046.67 (Figure 6b).

In the malignant tissue sample of patient 4, an enhanced quantity of iso-CD75s-gangliosides was detected by use of the AB2-3 antibody (Figure 6c and d). In the AB2-3 labeled upper band, $IV^3Neu5Ac-nLc4Cer$ (d18:1, C24:1/C24:0) is documented by the $[M_2 + 2Na - H]^+$ ions at m/z 1672.91/1674.91 together with low abundant $IV^3Neu5Ac-nLc4Cer$ (d18:1, C22:0) indicated by $[M_1 + 2Na - H]^+$ ions at m/z 1646.88 (Figure 6c). In the lower band, the corresponding iso-CD75s-ganglioside with C16:0 fatty

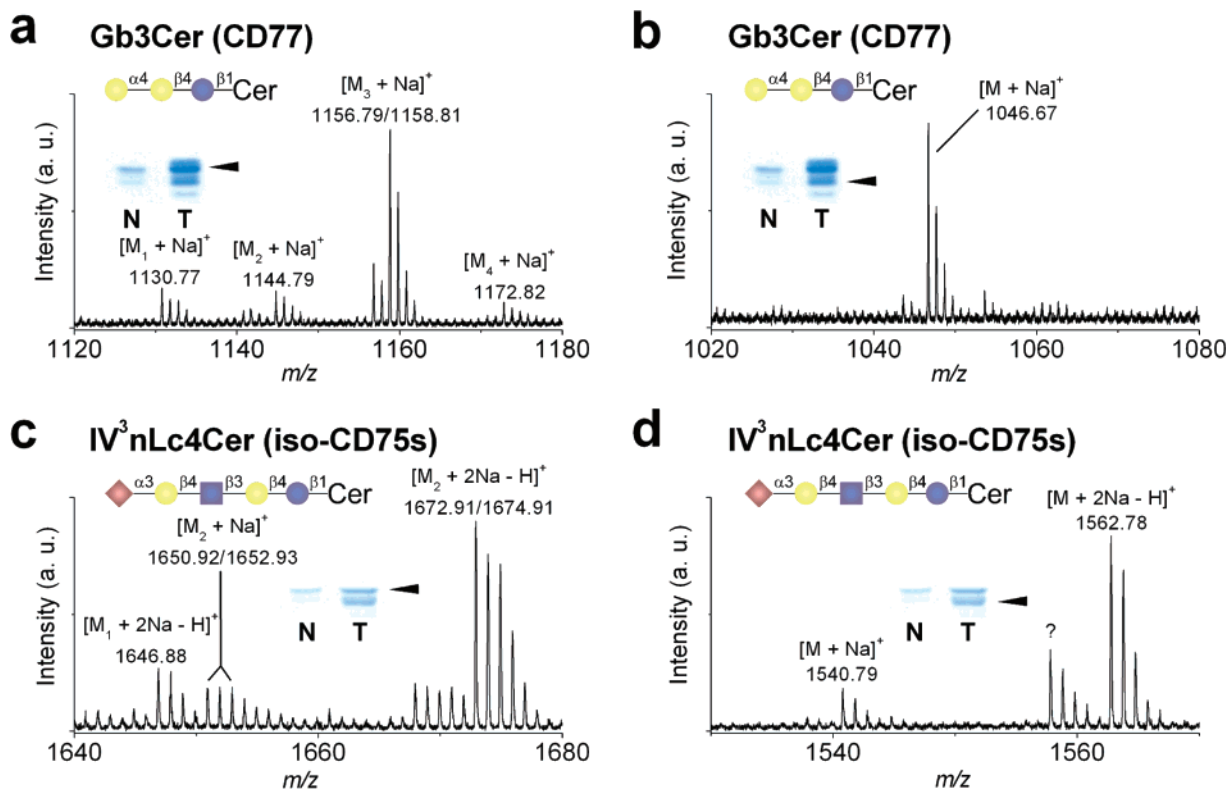


Figure 6. Tracing tumor-associated GSLs in pancreatic cancer. Aliquots from crude lipid extracts of normal (N) and tumor tissue (T) were separated simultaneously by TLC, immunostained, and the arrowhead marked tumor-associated GSLs analyzed by IR-MALDI-MS. (a, b) Patient 3. Extracts equivalent to 0.5 mg of wet weight tissue were applied and Gb3Cer probed with anti-Gb3Cer antibody. The prevalent $[M_3 + Na]^+$ ions in panel a correspond to Gb3Cer (d18:1, C24:1/C24:0) accompanied by minor $[M_1 + Na]^+$, $[M_2 + Na]^+$, and $[M_4 + Na]^+$ ions representing Gb3Cer (d18:1) with C22:0, C23:0, and C25:0 fatty acids according to their increasing m/z values. The $[M + Na]^+$ ions in panel b represent Gb3Cer (d18:1, C16:0). (c, d) Patient 4. Extracts equivalent to 3 mg of wet weight tissue were applied and iso-CD75s-gangliosides probed with antibody AB2-3. Dominant $[M_2 + 2Na - H]^+$ and low abundant $[M_2 + Na]^+$ ions in panel c correspond to IV3Neu5Ac-nLc4Cer (d18:1, C24:1/C24:0), and the minor $[M_1 + 2Na - H]^+$ ions to IV3Neu5Ac-nLc4Cer (d18:1, C22:0). The $[M + 2Na - H]^+$ and $[M + Na]^+$ ions in panel d represent IV3Neu5Ac-nLc4Cer (d18:1, C16:0). Type of molecular ions, m/z values, and proposed structures of GSLs are listed in Table S-5 of the Supporting Information. The basic histological characteristics of tumors are summarized in Table S-4 of the Supporting Information.

acid was detected in enhanced concentrations recorded by the $[M + 2Na - H]^+$ ions at m/z 1562.78 (Figure 6f).

The immunodetection of CD75s- and iso-CD75s-gangliosides in two hepatocellular tumors (Figure 5) and Gb3Cer and iso-CD75s-gangliosides in two pancreatic tumors (Figure 6) indicated enhanced expression in the malignant tissues compared to substantially lessened concentrations in the corresponding unaffected tissues of the patients. In general, identical molecular ions but with much lower signal intensities were detected by TLC-IR-MALDI-MS in the corresponding normal tissue samples. This is exemplarily shown for the iso-CD75s-gangliosides of the unaffected pancreas tissue of patient 4 in Figure S-5 of the Supporting Information.

Histological type, stage, and grading of the tumors are compiled in Table S-4 of the Supporting Information, and a synopsis of the proposed structures of the tumor-associated GSLs is provided in Table S-5 in the Supporting information, too. For technical reasons, i.e., because our *o*-TOF mass spectrometer is not equipped with a fragmentation facility, it should be mentioned that without MS/MS analysis a minute uncertainty regarding the composition of the ceramide moieties of the proposed structures remains left. Thus, the identified GSL structures of tumor-associated gangliosides and neutral GSLs represent their most likely structures. However, as a major outcome of this clinically

important investigation, we can summarize: (i) Crude lipid extracts are suitable for the structural analysis of tumor associated GSLs, and (ii) small-sized tissue samples of milligram quantities containing nanogram amounts of GSLs are sufficient for in situ TLC-IR-MALDI-MS.

DISCUSSION

The prerequisite for the application of TLC-MS to overlay-detected GSLs is the removal of the polymeric silica gel fixative (Plexigum) that would prevent the ionization process and the acquisition of mass spectra. Dipping the plate into chloroform (i) removes the plastic, but not the blue BCIP precipitate and (ii) leaves GSLs intact at the overlay-detected positions enabling an unambiguous assignment of protein-detected GSLs. This “trick” is also essential for indirect MS analysis of immunostained GSLs from silica gel extracts^{40,51} or direct UV-MALDI-MS as described for TLC-MS of immunostained asialo GM1.³⁵ The piggyback constructs of primary anti-GSL polyclonal and monoclonal antibodies, bacterial toxins, plant lectins, and the related antibodies in conjunction with the alkaline phosphatase-labeled antibodies and the blue BCIP precipitate did not interfere with MS analysis. Compared to the various indirect strategies for combining TLC

(51) Meisen, I.; Peter-Katalinić, J.; Müthing, J. *Anal. Chem.* **2004**, *76*, 2248–2255.

and MS performed by extraction of GSLs from the silica gel followed by MS analysis,^{40,51–54} direct TLC-MS has the advantage of omitting any extraction steps and of being less laborious.^{32–36,38,39} By direct TLC-MS, we previously aimed at the compositional mapping of GM3-variants³⁷ setting the starting point to develop the MS analysis of overlay-detected GSLs.

In a recent publication, Suzuki and colleagues³⁵ first showed the UV-MALDI-TLC-MS coupling for the analysis of immunostained asialo GM1 and demonstrated an MS/MS detection limit of ~60 ng. Compared to UV lasers, IR lasers offer the advantage of ablating more material per laser pulse on the order of a few micrometers in depth,^{37,39,55,56} which may facilitate the release of GSL molecules from the silica gel. In UV-MALDI, only analyte molecules incorporated in matrix crystals on top of the silica gel layer are desorbed, resulting in a rapid decline of ion signal with the number of applied laser pulses. This can explain the higher sensitivity of our IR laser approach resulting in detection limits of less than 1 ng at its best of antibody-detected neutral GSLs. A focus of our current research is the coupling of an IR-MALDI source to a high-resolution Fourier transform ion cyclotron resonance mass spectrometer. Besides the unsurpassed resolving power and mass accuracy of this type of mass analyzer,⁵⁷ MS/MS and even MSⁿ experiments should be achievable for TLC-MS³³ and may allow for an even more precise structural characterization due to generation of GSL fragment ions.

Our TLC-IR-MALDI-MS approach works with crude lipid extracts, omitting any laborious downstream procedures such as anion exchange chromatography (to separate neutral GSLs from negatively charged gangliosides) followed by silica gel adsorption chromatography or further purification by high-performance liquid chromatography⁵⁸ and preparative thin-layer chromatography to obtain single GSL fractions. Because coextracted phospholipids dominate in all cellular crude lipid extracts and influence the chromatography of GSLs by overloading the chromatogram and disturbing the separation, phospholipids were saponified followed by dialysis to desalt the sample representing the only “purification step” required for in situ TLC-IR-MALDI-MS. Clearance of phospholipid-derived breakdown products (mostly fatty acids) is simply obtained by TLC whereby fatty acids run ahead of the GSLs at the solvent frontier. Owing to the handling with total lipid extracts, (i) the risk of losing any GSLs that may occur through common downstream purification procedures is minimized and (ii) the GSL analysis is facilitated by investigating only one master lane containing the entire “glycosphingolipidome” of a certain cell type, tissue, or organ.

The lowest quantity of tissue extracted so far corresponded to 2 mg of wet weight of human pancreas, resulting in appropriate spectra in accord with those shown in this paper. These promising results will stimulate us to further downscaling of the technique to biopsy sample size aimed at the identification of tumor-

associated GSLs at the early stage of cancer development to be applied in preoperative diagnosis. In search of cancer-associated GSLs with therapeutic background,⁵⁹ the CD75s-gangliosides represent potential targets for adjuvant anticancer therapies with humanized monoclonal antibodies and native or recombinant lectins from plants.^{14,15} Even bacterial toxins with certain GSL-binding specificities, for example, the family of Gb3Cer (CD77) recognizing Stx1, Stx2, and their subtypes,⁶⁰ are currently under discussion as potential antitumor therapeutics.^{12,13}

New glycomic approaches are contributing to our increased understanding of the underlying biology that is responsible for the development of cancer and other diseases.⁶¹ The field of functional glycomics is now being explored through glycan array technology to decipher the information content of the glycome, i.e., the full carbohydrate repertoire of cells, tissue, and organs.^{62–66} The implementation of the neoglycolipid technology⁶⁷ was a milestone for the fabrication of glyco arrays, based on the oligosaccharide transfer from glycoconjugates to an acceptor lipid such as phosphatidylethanolamine. Neoglycolipids are readily amenable to numerous assay procedures established for natural GSLs, e.g., the TLC-binding technique⁶⁸ or direct analysis on chromatograms by liquid secondary ion mass spectrometry.^{31,69} Depending on the complexity of GSLs, deconvolution strategies can be carried out, which will end up in TLC-MS to determine the oligosaccharides that have been bound by a protein.^{63,64} In this context, our exceedingly sensitive TLC-IR-MALDI-MS analysis of overlay-detected GSLs represents a key starting point to interface the microarrays with mass spectrometry. In the foreseeable future, there is a need for miniaturization and automation of GSL separation and TLC-MS-coupled detection for the high-throughput array construction. Technically important, a wide range of liquid matrixes like glycerol or triethanolamine is available for IR-MALDI-MS on silica gel layers, which provide a well homogeneous preparation and would facilitate an automated analysis and target miniaturization of the TLC overlay procedure, but the technology is only at its beginning.

CONCLUSIONS

The in situ TLC-IR-MALDI-MS technology merging TLC, immunodetection, and MS opens new doors for the developing field of functional glycomics by delivering structural information of trace quantities of GSLs with only a limited investment in sample purification. A major challenge facing glycomics and its clinical applications will be the ability to accurately profile the glycosylation stage of a patient to identify the type of disease and, based on this profile, to determine the appropriate treatment for the individual patient. All in all, we hypothesize that this powerful

- (52) Stroud, M. R.; Stapleton, A. E.; Levery, S. *Biochemistry* **1998**, *37*, 17420–17428.
- (53) Hildebrandt, H.; Jonas, U.; Ohashi, M.; Klaiber, I.; Rahmann, H. *Comp. Biochem. Physiol. B. Biochem. Mol. Biol.* **1999**, *122*, 83–88.
- (54) Niimura, Y.; Ishizuka, I. *Glycobiology*, **2006**, *16*, 729–735.
- (55) Dreisewerd, K. *Chem. Rev.* **2003**, *103*, 395–425.
- (56) Berkenkamp, S.; Kirpekar, F.; Hillenkamp, F. *Science* **1998**, *281*, 260–262.
- (57) Vukelić, Ž.; Zamfir, A. D.; Bindila, L.; Froesch, M.; Peter-Katalinić, J. *J. Am. Soc. Mass Spectrom.* **2005**, *16*, 571–580.
- (58) Müthing, J. *Methods Enzymol.* **2000**, *312*, 45–64.

- (59) Fredman, P.; Hedberg, K.; Brezicka, T. *BioDrugs* **2003**, *17*, 155–167.
- (60) Bielaszewska, M.; Karch, H. *Thromb. Haemostasis* **2005**, *94*, 312–318.
- (61) Miyamoto, S. *Curr. Opin. Mol. Ther.* **2006**, *6*, 507–513.
- (62) Feizi, T. *Glycoconjugate J.* **2000**, *17*, 553–565.
- (63) Fukui, S.; Feizi, T.; Galustian, C.; Lawson, A. M.; Chai, W. *Nat. Biotechnol.* **2002**, *20*, 1011–1017.
- (64) Feizi, T.; Chai, W. *Nat. Rev. Mol. Cell Biol.* **2004**, *5*, 582–588.
- (65) Morelle, W.; Michalski, J. C. *Curr. Pharm. Des.* **2005**, *11*, 2615–2645.
- (66) Pilobello, K. T.; Mahal, L. K. *Curr. Opin. Chem. Biol.* **2007**, *11*, 300–305.
- (67) Feizi, T.; Stoll, M.; Yuen, C.-T.; Chai, W.; Lawson, A. M. *Methods Enzymol.* **1994**, *230*, 484–519.
- (68) Magnani, J. L.; Spitalnik, S. L.; Ginsburg, V. *Methods Enzymol.* **1987**, *138*, 195–207.
- (69) Lawson, A. M.; Chai, W. G.; Cashmore, G. C.; Stoll, M. S.; Hounsell, E. F.; Feizi, T. *Carbohydr. Res.* **1990**, *200*, 47–57.

technology will truly find its place in the emerging field of “glycosphingolipidomics” and hopefully contribute to a successful fight against life threatening diseases like cancer.

ACKNOWLEDGMENT

This work is currently funded by the Deutsche Krebshilfe (grant DKH 106742) and the Deutsche Forschungsgemeinschaft (DFG, grants FR2569/1-1 and MU845/4-1) and has been supported by DFG grant DR416-5/1. The authors thank Sequenom

GmbH (Hamburg, Germany) for providing use of their o-TOF instrument.

SUPPORTING INFORMATION AVAILABLE

Additional information as noted in text. This material is available free of charge via the Internet at <http://pubs.acs.org>.

Received for review October 8, 2007. Accepted January 10, 2008.

AC702071X